ELEMENTAL COMPOSITION DIAGNOSTICS FOR HINODE/EIS

Hinode 15 / IRIS 12

Natalia Zambrana Prado
S. Parenti & the ISSI team #418
P. Young, T. Kucera,
É. Buchlin, G. Pelouze
NASA Goddard Space Flight Center
Institut d'Astrophysique Spatiale

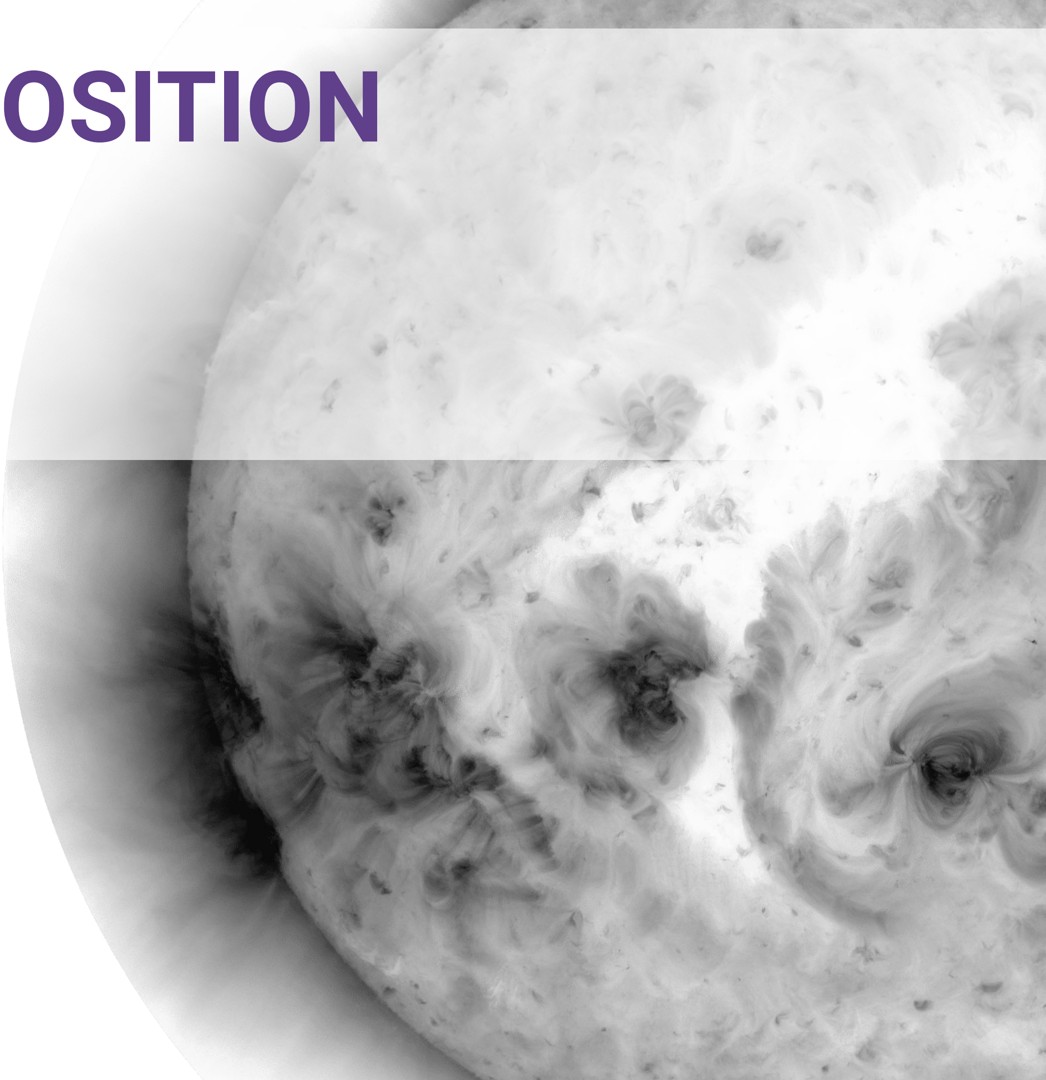

The FIP effect

Relative elemental composition measurement in the slow solar wind (von Steiger et al., 1997).

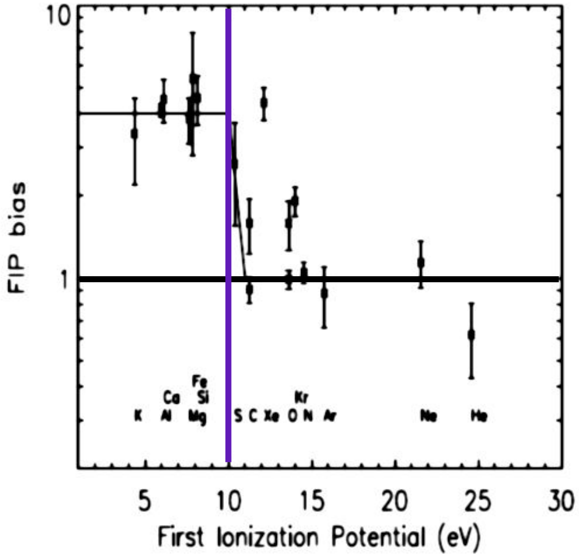

abundance enhancement

$$\frac{Ab^{corona}}{Ab^{photosphere}} = \text{FIP bias}$$

photospheric abundances

FIP bias map of the Solar corona, Brooks et al. (2014)

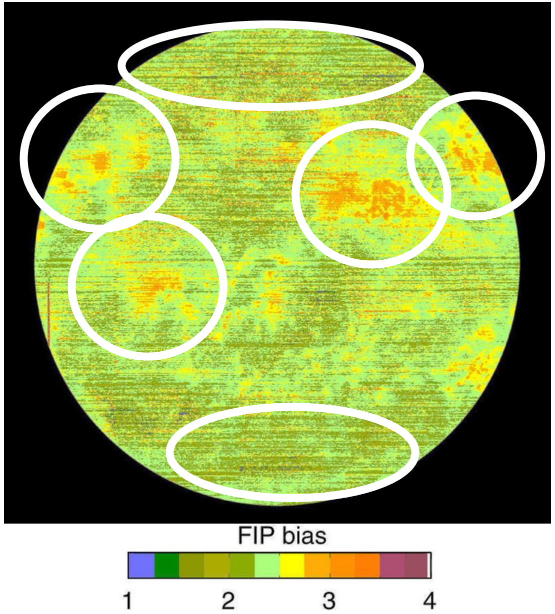

FIP bias set in the chromosphere and then frozen in high corona

FIP biases measurements give constraints on the source of heliospheric plasma

Linking the Sun to the Heliosphere

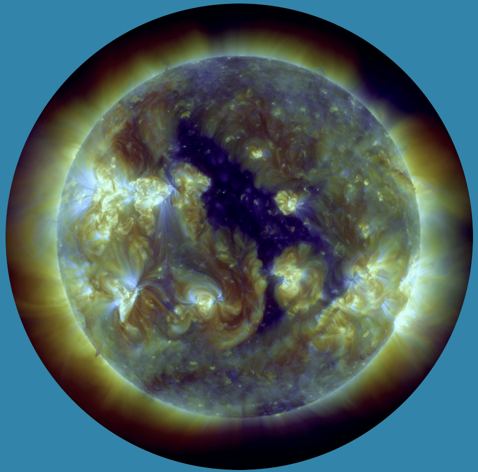

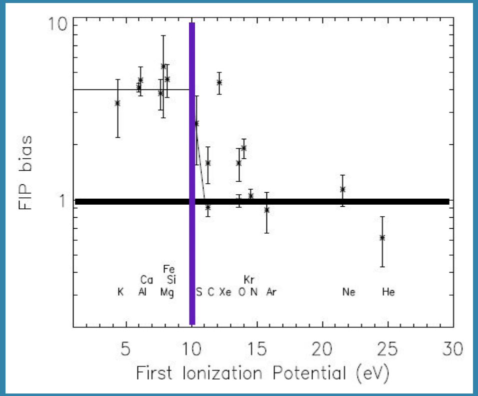

FIP bias maps in the corona ← Remote sensing (EUV spectroscopy)

Comparisons ↕ Modeling

(+ magnetic field, velocities)

Abundance measurements in the Solar Wind ← In-situ measurements

FIP bias diagnostics: Linear Combination Ratio (LCR)

Zambrana Prado & Buchlin (2019)

- Starting from the relative FIP bias: $\frac{f^{bias}_{X_{\mathrm{LF}}}}{f^{bias}_{X_{\mathrm{HF}}}} = \frac{I_{\mathrm{LF}}}{I_{\mathrm{HF}}} \left(\frac{A^{\mathrm{ph}}_{X_{\mathrm{LF}}}}{A^{\mathrm{ph}}_{X_{\mathrm{HF}}}} \frac{\langle C_{\mathrm{LF}}, \mathrm{DEM}\rangle}{\langle C_{\mathrm{HF}}, \mathrm{DEM}\rangle} \right)^{-1}$ = constant
- We select linear combinations of lines from low- and high-FIP elements, one from low-FIP element(s) and one from high-FIP element(s)
- We optimize the coefficients of these linear combinations to get the ratio of "scalar products" to be as closed as possible to 1, for different reference DEMs

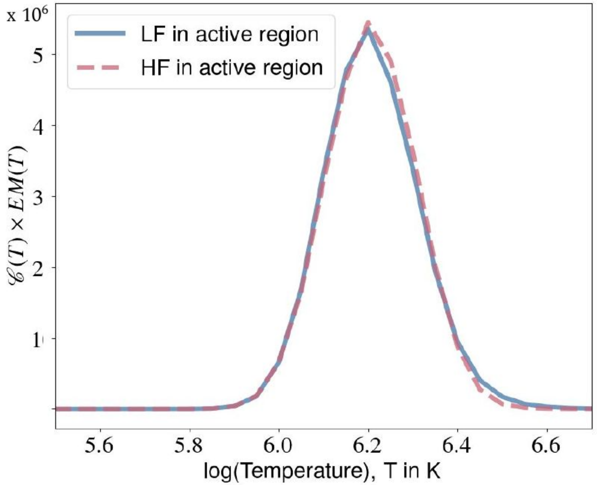

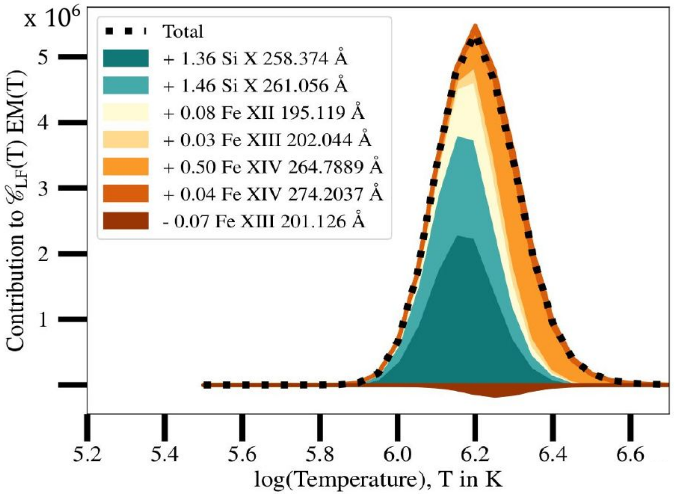

QS	1.000008
AR	1.000004
CH	0.999991

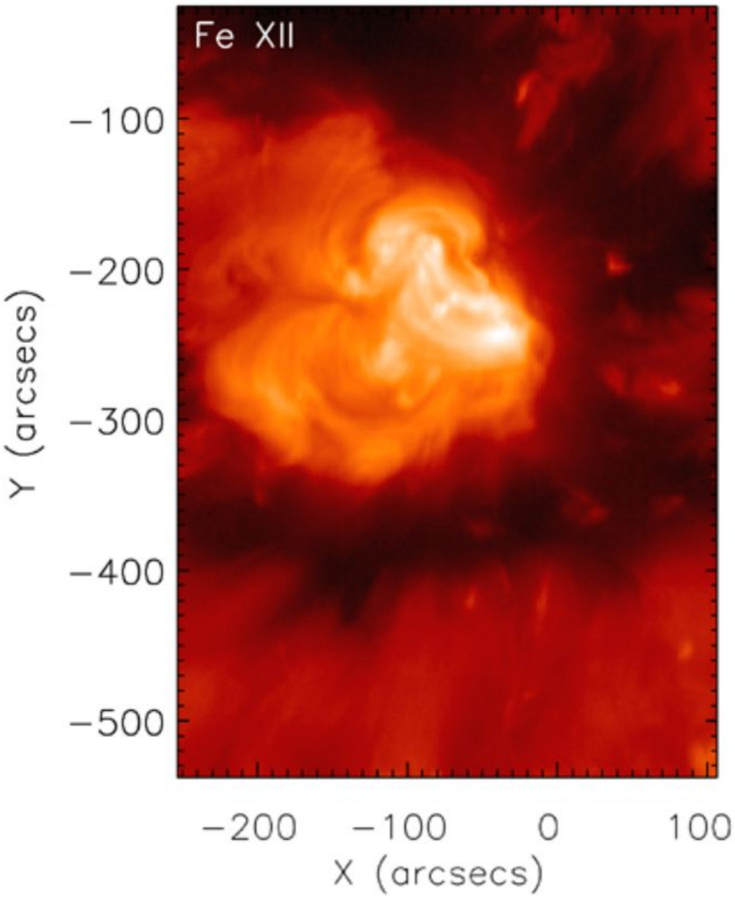

Fe XII intensity map of the AR observed with EIS on 17 October 2007 at 02:47 UT, Baker et al. 2012

In practice : Hinode/EIS

Application of the LCR method to spectroscopic observations of a sigmoidal anemone-like Active Region inside an equatorial Coronal Hole, previously studied in Baker et al. (2013).

Following DEM inversion

$$\frac{f_{\mathrm{Si}}}{f_{\mathrm{S}}}$$

Linear combinations

$$\frac{f_{\mathrm{Si\ \&\ Fe}}}{f_{\mathrm{S}}}$$

In practice : Hinode/EIS

Application of the LCR method to spectroscopic observations of a sigmoidal anemone-like Active Region inside an equatorial Coronal Hole, previously studied in Baker et al. (2013).

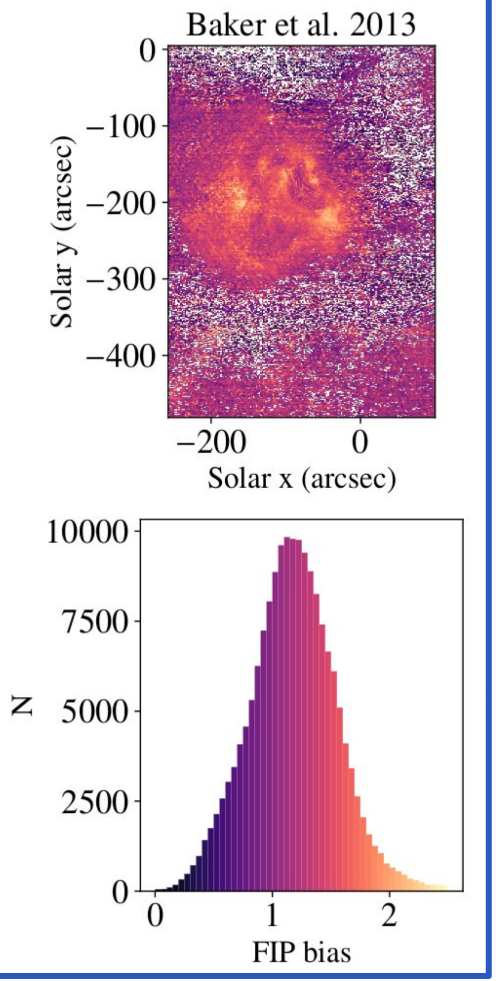

Data courtesy of D. Baker

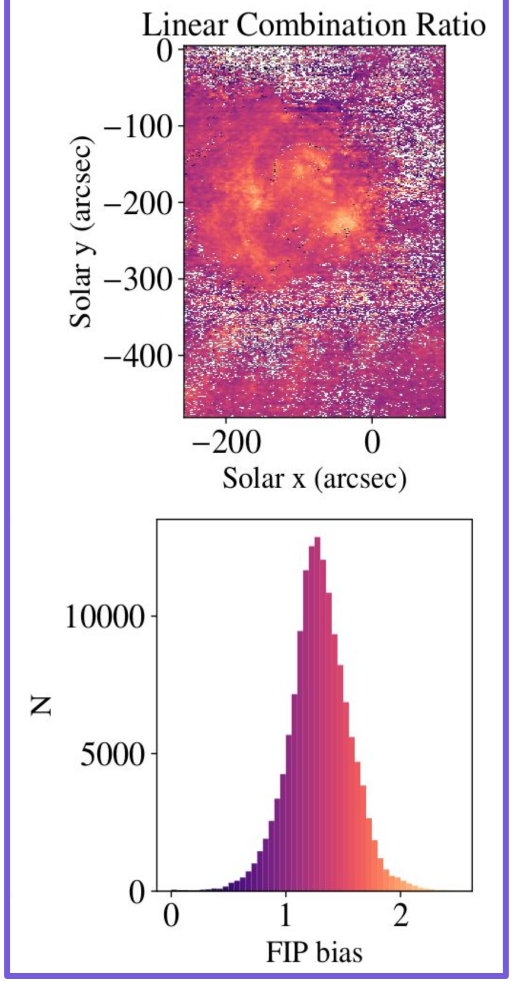

Zambrana Prado & Buchlin, 2019

Following DEM inversion

$$\frac{f_{\mathrm{Si}}}{f_{\mathrm{S}}}$$

Linear combinations

$$\frac{f_{\mathrm{Si\ \&\ Fe}}}{f_{\mathrm{S}}}$$

★ Similar structures with enhanced or depleted relative FIP bias in both maps.

White pixels: warm or dead pixels + too noisy to fit the spectral line properly

Reanalyzing past observations with the LCR method

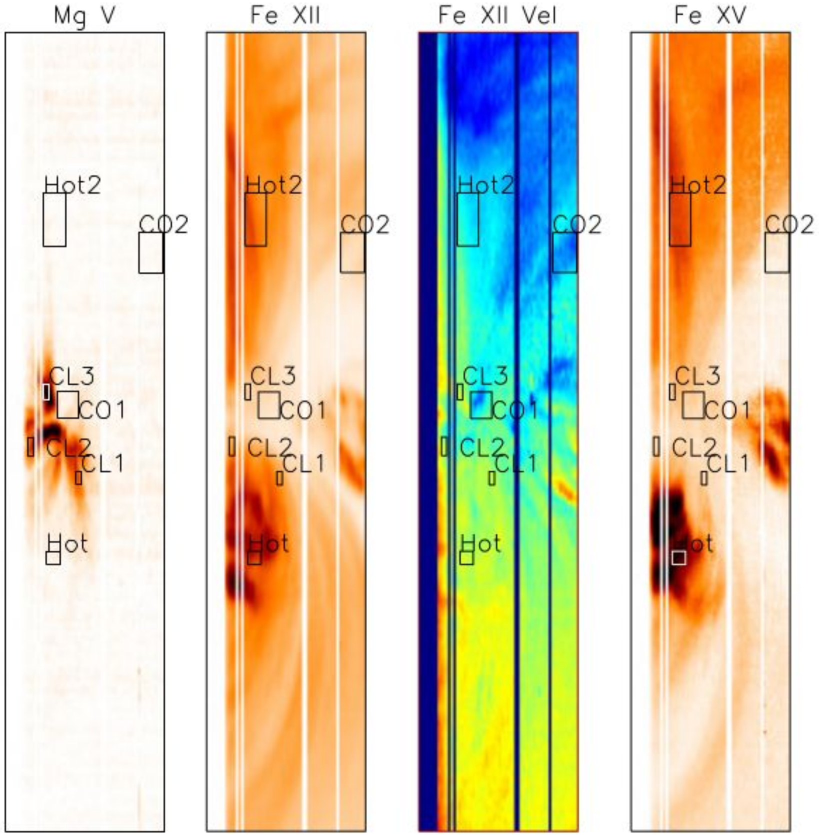

Parenti et al. (including NZP), 2021

Set #	Ion	Wavelength (Å)	log T_{max} (K)
1	**S VIII**	**198.553**	5.9
	Si VII	275.361	5.8
	Si VIII	276.85	5.9
	Fe X	184.537	6.0
	Fe XI	180.401	6.1
2	**S X**	**264.23**	6.2
	Si X	258.374	6.1
	Fe XIII	202.044	6.2
	Fe XIV	264.788	6.3
3	**S XII**	**288.434**	6.3
	S XIII	**256.685**	6.4
	Fe XV	284.163	6.3
	Fe XIV	211.317	6.3
	Fe XVI	262.976	6.4
4	**Ar XIV**	**194.401**	6.5
	Ca XIV	193.866	6.5
	Fe XV	284.163	6.3

Reanalyzing past observations with the LCR method

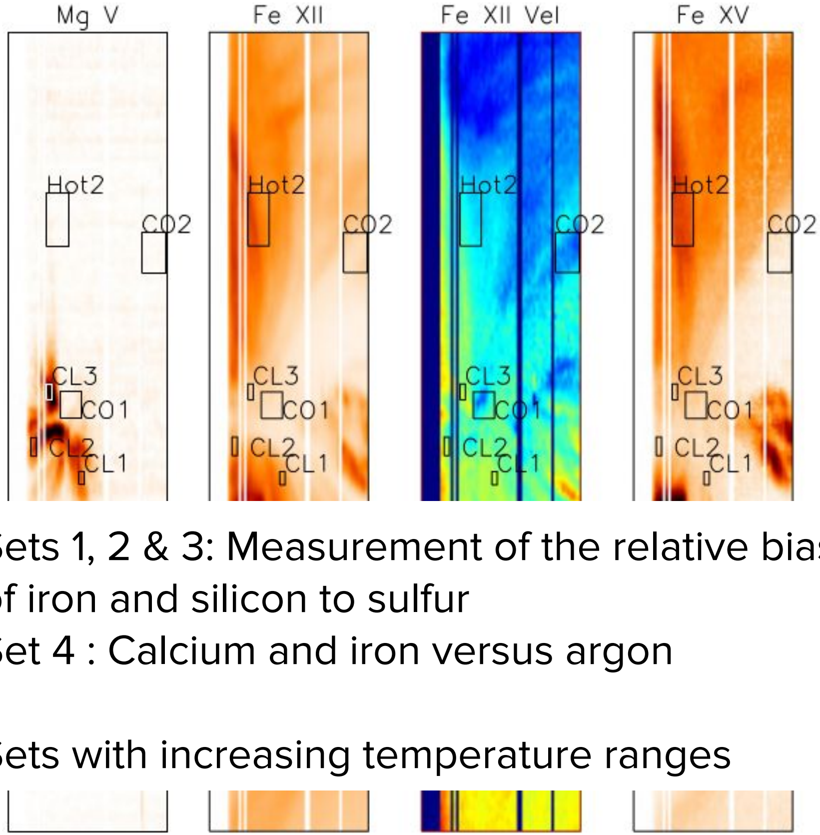

Sets 1, 2 & 3: Measurement of the relative bias of iron and silicon to sulfur
Set 4 : Calcium and iron versus argon

Sets with increasing temperature ranges

Parenti et al. (including NZP), 2021

Set #	Ion	Wavelength (Å)	log T_{max} (K)
1	**S VIII**	**198.553**	5.9
	Si VII	275.361	5.8
	Si VIII	276.85	5.9
	Fe X	184.537	6.0
	Fe XI	180.401	6.1
2	**S X**	**264.23**	6.2
	Si X	258.374	6.1
	Fe XIII	202.044	6.2
	Fe XIV	264.788	6.3
3	**S XII**	**288.434**	6.3
	S XIII	**256.685**	6.4
	Fe XV	284.163	6.3
	Fe XIV	211.317	6.3
	Fe XVI	262.976	6.4
4	**Ar XIV**	**194.401**	6.5
	Ca XIV	193.866	6.5
	Fe XV	284.163	6.3

Reanalyzing past observations with the LCR method

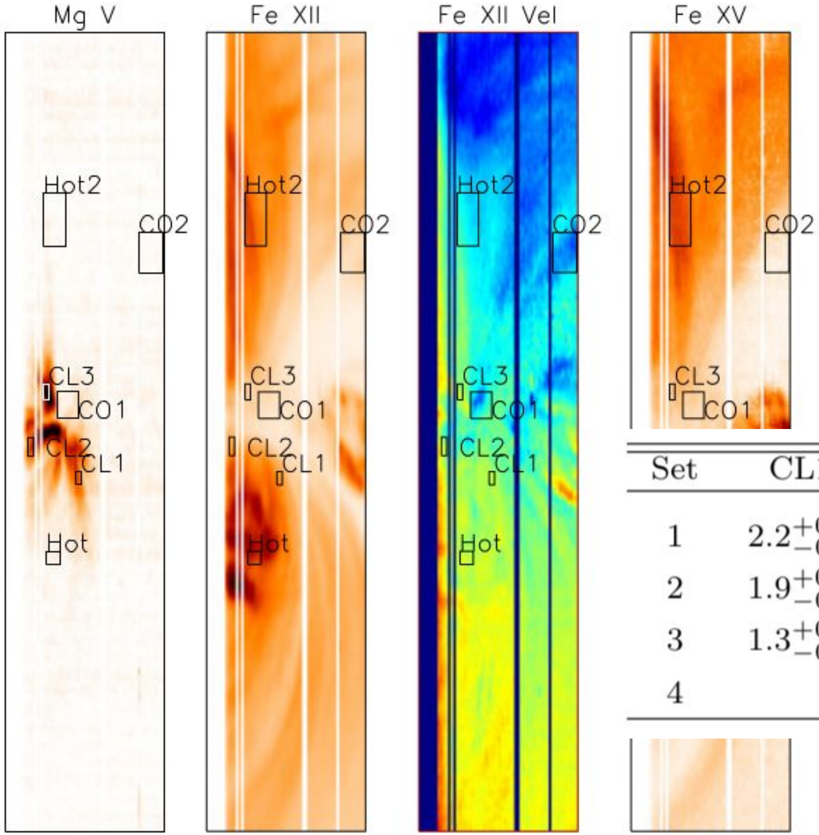

Sets with **increasing temperature ranges**

Sets 1, 2 & 3: Measurement of the relative bias of iron and silicon to sulfur

Set 4 : Calcium and iron versus argon

Set	CL1	CL2	CL3	CO1	CO2	HOT	HOT2
1	$2.2^{+0.8}_{-0.7}$	$2.7^{+0.9}_{-0.8}$	$2.7^{+0.9}_{-0.8}$	$2.0^{+0.7}_{-0.6}$	$1.8^{+0.6}_{-0.6}$	$1.0^{+0.4}_{-0.3}$	$0.9^{+0.3}_{-0.3}$
2	$1.9^{+0.6}_{-0.5}$	$1.6^{+0.5}_{-0.4}$	$2.0^{+0.6}_{-0.5}$	$2.0^{+0.6}_{-0.5}$	$2.0^{+0.6}_{-0.5}$	$1.7^{+0.5}_{-0.5}$	$1.9^{+0.6}_{-0.5}$
3	$1.3^{+0.7}_{-0.1}$			$2.5^{+1.5}_{-0.0}$	$1.8^{+1.0}_{-0.0}$	$1.8^{+1.0}_{-0.0}$	$1.4^{+0.9}_{-0.0}$
4				$3.1^{+1.6}_{-0.3}$	$3.3^{+1.5}_{-0.2}$		

Parenti et al. (including NZP), 2021

Sources of error

Specific to the **LCR method** :

- ★ Minimized cost function is not equal to zero.
- ★ The DEMs in the map are different from the ones we used for the optimization.
- ★ Mixing of elements with different FIP biases

Other sources of error :

- ★ Radiometry
- ★ Atomic physics
- ★ Radiative transfer

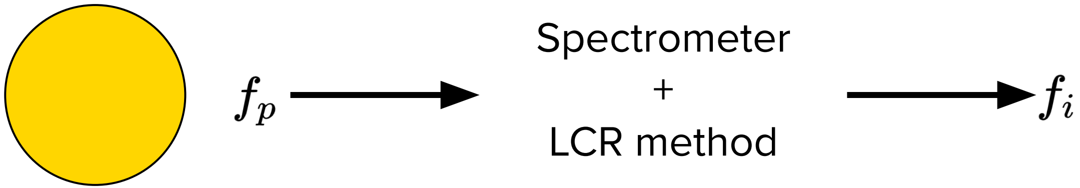

→ There is a difference between the **real relative FIP bias** of the plasma f_p and the **inferred relative FIP bias** obtained from observations f_i

Determining uncertainties from the probability distribution $P(f_p \mid f_i)$

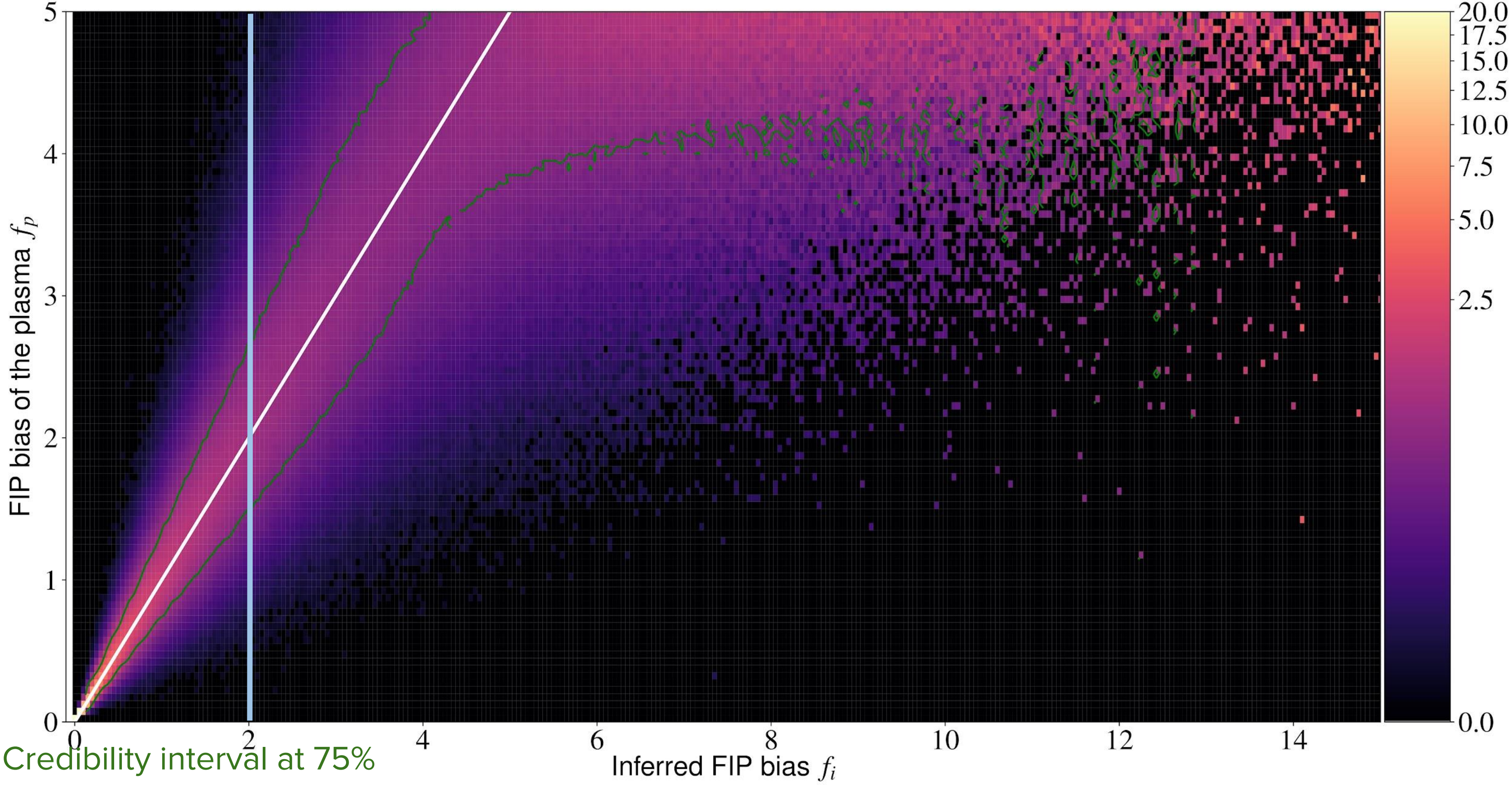

Credibility interval at 75%

Determining uncertainties from the probability distribution $P(f_p \mid f_i)$

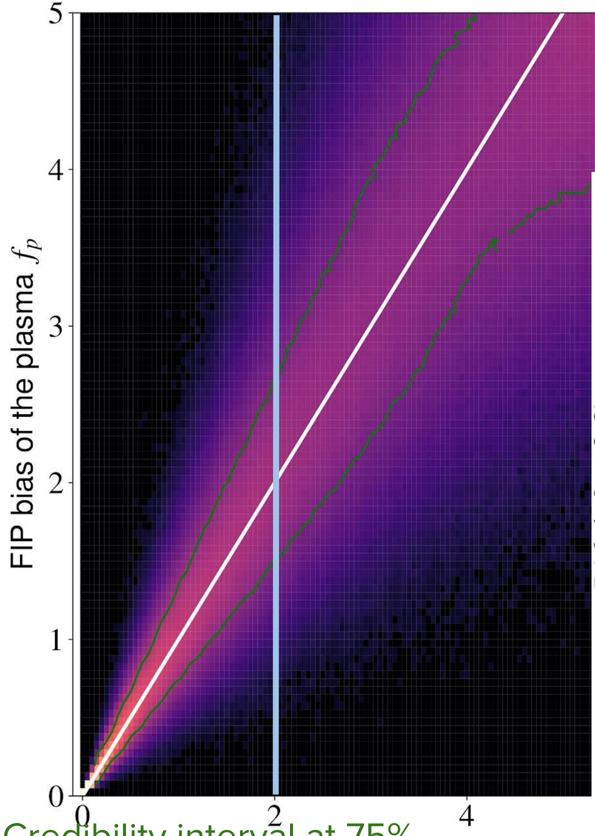

Credibility interval at 75%

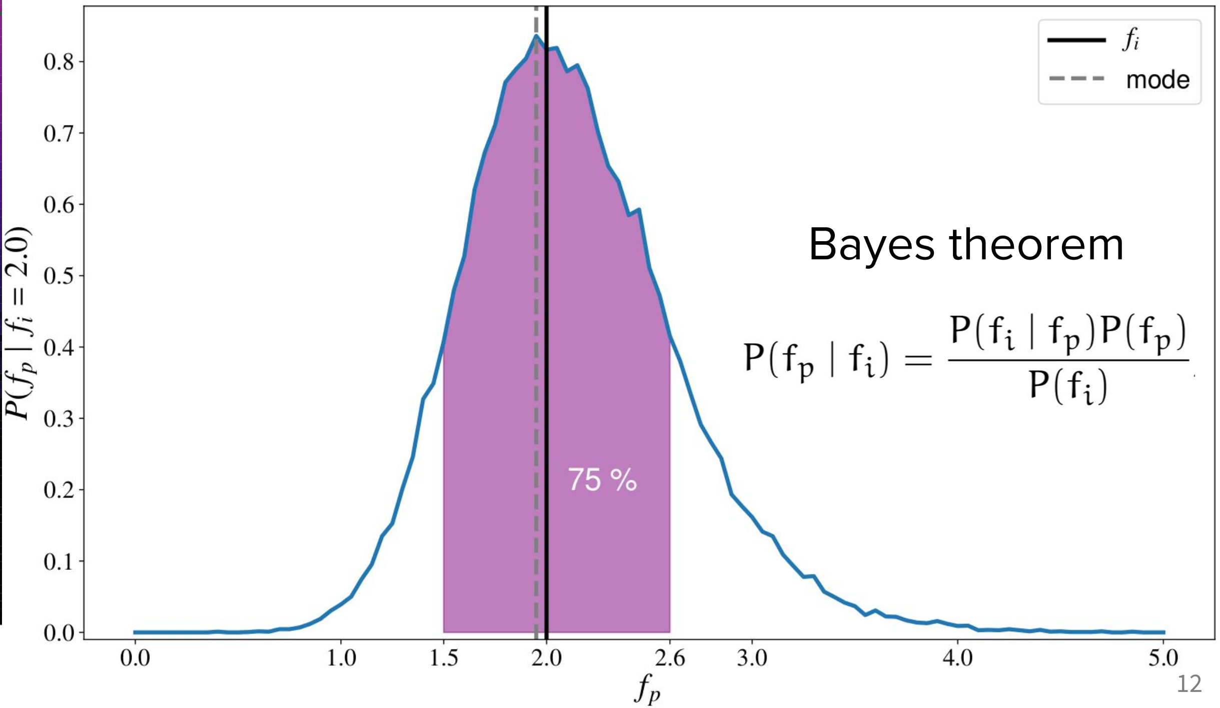

Bayes theorem

$$P(f_p \mid f_i) = \frac{P(f_i \mid f_p)P(f_p)}{P(f_i)}$$

Moving forward: EIS & Solar Orbiter

- ★ EIS has more LF lines whereas SPICE has more HF lines
- ★ Coordinated observations allow for a better constraint on the higher temperature range for SPICE and provide Doppler maps.
- ★ EIS observes more iron lines which is one of the heavy ions SWA-HIS measures.
- ★ Possibility to understand what is happening at different temperatures and heights.

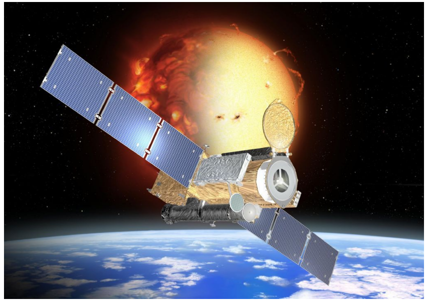

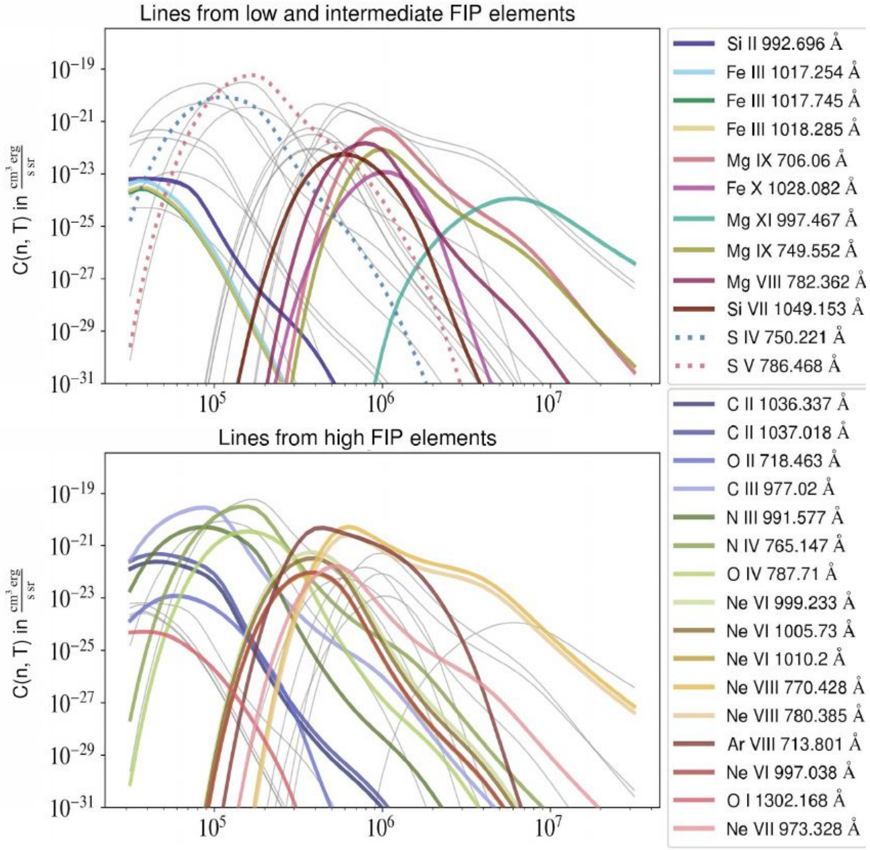

What we have

Spectroscopic observations

How

A **new FIP bias measuring method** with:

- ★ No DEM Inversion
- ★ Optimized linear combinations of spectral lines

What we want to do

- ★ Create accurate FIP bias maps systematically and semi-automatically
- ★ Re-analyze past observations
- ★ Design observations : which lines should we use ?

All routines in Python available at
https://git.ias.u-psud.fr/nzambran/fiplcr

Conclusions

- FIP bias measurements give **constraints on the source of heliospheric plasma** (even if they are not enough to identify it: Stansby et al. 2020).
- **New diagnostics** at higher temperatures.
- New sets of spectral lines will add elemental composition diagnostics to previously carried out studies : **new EIS composition data product**.
- Application to **SPICE** observations.

Thank you for listening

zambranaprado@cua.edu
natalia.zambranaprado@nasa.gov